Annals of Botany **121**: 797–807, 2018
doi:10.1093/aob/mcx100, available online at www.academic.oup.com/aob

ANNALS OF BOTANY
Founded 1887

PART OF A SPECIAL ISSUE ON FUNCTIONAL–STRUCTURAL PLANT GROWTH MODELLING

High light aggravates functional limitations of cucumber canopy photosynthesis under salinity

Tsu-Wei Chen[1,*], Hartmut Stützel[1] and Katrin Kahlen[2]

[1]Institute of Horticultural Production Systems, Leibniz Universität Hannover, Herrenhäuser Straße 2, 30419 Hannover, Germany and [2]Geisenheim University, Von-Lade-Straße 1, 65366 Geisenheim, Germany
**For correspondence. E-mail chen@gem.uni-hannover.de*

Received: 24 April 2017 Returned for revision: 8 June 2017 Editorial decision: 26 June 2017 Accepted: 24 July 2017
Published electronically 19 September 2017

• **Background and Aims** Most crop species are glycophytes, and salinity stress is one of the most severe abiotic stresses reducing crop yields worldwide. Salinity affects plant architecture and physiological functions by different mechanisms, which vary largely between crop species and determine the susceptibility or tolerance of a crop species to salinity.
• **Methods** Experimental data from greenhouse cucumber (*Cucumis sativus*), a salt-sensitive species, grown under three salinity levels were interpreted by combining a functional–structural plant model and quantitative limitation analysis of photosynthesis. This approach allowed the quantitative dissection of canopy photosynthetic limitations into architectural and functional limitations. Functional limitations were further dissected into stomatal (L_s), mesophyll (L_m) and biochemical (L_b).
• **Key Results** Architectural limitations increased rapidly after the start of the salinity treatment and became stronger than the sum of functional limitations ($L_s + L_m + L_b$) under high salinity. Stomatal limitations resulted from ionic effects and were much stronger than biochemical limitations, indicating that canopy photosynthesis was more limited by the effects of leaf sodium on stomatal regulation than on photosynthetic enzymes. Sensitivity analyses suggested that the relative importance of salinity effects on architectural and functional limitations depends on light conditions, with high light aggravating functional limitations through salinity effects on stomatal limitations.
• **Conclusions** Salinity tolerance of cucumber is more likely to be improved by traits related to leaf growth and stomatal regulation than by traits related to tissue tolerance to ion toxicity, especially under high light conditions.

Keywords: Canopy photosynthesis, FvCB model, quantitative limitation analysis, *Cucumis sativus*, functional–structural plant model, architecture, salinity, stress combination, high light.

INTRODUCTION

Salinity stress is one of the most severe abiotic stresses reducing crop yields worldwide (Munns and Tester, 2008). It affects both plant architecture and physiological functions. Typical salinity effects on whole plant architecture are a reduction in organ size, e.g. leaf area (Rawson and Munns, 1984; Rajendran *et al.*, 2009), which limits canopy light interception, and affects light distribution within the canopy and the size of the photosynthetic apparatus (referred to as architectural limitations). Salt in the soil and salt accumulation in the leaves (mainly Na^+; Savvas *et al.*, 2005; Stępień and Kłobus, 2006; Pérez-López *et al.*, 2012) disturb stomatal regulation, increase diffusional resistance to CO_2 transport to the chloroplast, and reduce biochemical capacity and light use efficiency (referred to as functional limitations). Architectural and functional limitations of salinity reduce whole plant photosynthesis and consequently crop yields.

In the literature, speculations about the relative importance of different mechanisms related to architectural and functional limitations can be found. For example, it has been proposed that the reduction of leaf area and stomatal closure due to the osmotic components of salinity have greater impact on growth than physiological disturbances due to ion accumulation in the plant (Munns and Tester, 2008). In contrast, it has also been proposed that ion exclusion and tolerance to toxic ions in leaves are the main mechanisms maintaining plant growth under salinity (Rajendran *et al.*, 2009). The prevailing opinion is that stomatal conductance constitutes the primary photosynthetic limitation under salinity (Centritto *et al.*, 2003; Flexas *et al.*, 2004; Pérez-López *et al.*, 2012), while there are data showing that biochemical limitations are equally or even more prominent than stomatal limitations (Drew *et al.*, 1990; Chen *et al.*, 2015a). Despite these different opinions about the relative impacts of different physiological effects of salinity, no quantitative assessment of these impacts at the whole plant level exists in the literature, except for one study dissecting the combined effects of salinity and high temperature into architectural and functional limitations by combining a dynamic architectural model of tomato with a simple light response of photosynthesis (Chen *et al.*, 2015b). By using a more sophisticated biochemical model of photosynthesis (Farquhar *et al.*, 1980), it is possible to further dissect the functional limitations quantitatively into stomatal, mesophyll and biochemical (Grassi and Magnani, 2005). This approach, referred to as quantitative limitation analysis, has been demonstrated to be a useful tool for dissecting the contributions of physiological parameters

to photosynthetic limitations under saturating light conditions (Egea *et al.*, 2011; Flexas *et al.*, 2013; Cano *et al.*, 2013). Recently, quantitative limitation analysis has been extended to non-saturating light conditions (Chen *et al.*, 2014a) and to partition photosynthetic limitation into more variables (Buckley and Diaz-Espejo, 2015). These new approaches allow us to study the effects of diurnal and seasonal climatic variations on photosynthetic limitations and to up-scale photosynthetic limitations from leaf to canopy level by implementing them in a functional–structural plant model (FSPM). In a canopy, there are drastic gradients and heterogeneity of light and variations in leaf functional traits (Niinemets, 2012), which have complex effects on the composition of photosynthetic limitations at the leaf level (Chen *et al.*, 2015a). This is in agreement with both theoretical (Chen *et al.*, 2014a) and experimental (Cano *et al.*, 2013) results showing that the composition of photosynthetic limitations varies between different canopy layers. Furthermore, canopy architecture responds to environmental stress in a dynamic way, which should be taken into account when quantifying the impact of architectural traits on canopy photosynthesis (Chen *et al.*, 2014b).

Altogether, different opinions about the relative importance of physiological mechanisms on salinity tolerance might have been due to the complex interactions between stress and environmental conditions, plant architecture and physiological functions, since the stress tolerance conferred by a certain trait may vary depending on the environmental scenario (Tardieu, 2012). In this work, we built FSPMs based on digitized cucumber canopies throughout a greenhouse experiment with three salinity levels and a validated leaf photosynthesis model. These FSPMs allowed us to interpret the salinity effects on cucumber growth in that experiment in the context of architectural and functional limitations. We further dissected the functional limitations into stomatal, mesophyll, biochemical and light limitations. This approach aims to give a systematic understanding of the important traits conferring salinity tolerance at different developmental stages, under different light environments and severity of salinity.

MATERIALS AND METHODS

Plant material and experimental design

Cucumber seeds (*Cucumis sativus* 'Aramon' Rijk Zwaan, De Lier, the Netherlands) were sown in rock-wool cubes (36 × 36 × 40 mm) on 12 June 2013. Seven days after sowing, seedlings were transplanted into larger rock-wool cubes (10 × 10 × 6.5 cm). On 25 June, plants were transplanted on rock-wool slabs (Grodan, Grodania A/S, Hedehusene, Denmark) in two greenhouses (two replications) of the Institute of Horticultural Production Systems, Leibniz Universität Hannover, Germany (52°23′N, 9°37′E). The greenhouses were heated to maintain 22/20 °C day/night temperature and roof ventilation was opened when the inside temperature was higher than 24 °C during the whole experiment. Each litre of the standard nutrient solution contained 0.5 g Ferty Basisdünger 2 (Planta GmbH, Regenstauf, Germany, 0.9 mM NO_3^-, 1.5 mM NH_4^-, 2.8 mM K^+, 3.0 mM Ca^{2+}, 0.4 mM Mg^{2+}, 0.4 mM H_2PO_4, as well as adequate amounts of the micronutrients) and extra 0.9 g $Ca(NO_3)_2$ was added to the solution (5.5 mM Ca^{2+} and 11 mM NO_3^-) after the first fruit set.

In each greenhouse, 50 cucumber plants were grown in five rows (orientated north–south), with plant and row distances equal to 60 and 120 cm, respectively. The plants of the left and right border rows were not used for measurements and irrigated with the standard nutrient solution. Three different salinity levels, obtained by adding 0, 25 and 50 mM NaCl to the standard nutrient solution, were randomly applied to the three rows in the middle on 8 July 2013. The northernmost and southernmost plants in the three middle rows were also considered border plants and were not used for measurements. All side shoots were removed to maintain monopodial growth and plants were decapitated at the 25th leaf to maintain a canopy height of 2 m. Whole plants were harvested on day 35 after exposure to salinity (DAS). Leaf area (measured by LI-COR 3100 area meter, LI-COR, Lincoln, NE, USA), and fresh weight of leaves, fruits, internodes and petioles were measured. Dry weights were measured after drying at 70 °C for at least 72 h. Weather data during the experiment were recorded by sensors above and inside the greenhouse (see Supplementary Data Fig. S1).

Reconstructing 3-D cucumber canopies to obtain light interception at the leaf level

The architectures of cucumber plants were digitized weekly using a 3-D digitizer (Fastrak, Polhemus, Colchester, VT, USA). For internodes, petioles and fruits, the 3-D coordinates of the beginning and end points were recorded and their lengths were calculated by these coordinates. For leaves, 13 points per leaf lamina were digitized. Using these points, a leaf lamina was reconstructed with 10 predefined triangles (Wiechers *et al.*, 2011). Three plants per salinity level were digitized on 0, 7, 14, 21, 28 and 35 DAS. At the end of the experiment, the leaf area measured with a leaf area meter and the areas estimated by plant digitization were compared to ensure the accuracy of plant digitization.

Using the digitized data, cucumber plants were reconstructed in *GroIMP* (Kniemeyer, 2008) according to Chen *et al.* (2014a). For setting up the virtual canopy structure, 50 cucumber plants were distributed in five rows. Distances between virtual plants in a row and between rows were 60 and 120 cm, respectively, as in the experiment (1.39 plants m^{-2}). Two reconstructed one-row canopies are shown in Supplementary Data Fig. S2. To simulate the light environment, the virtual canopy was surrounded by sun and sky providing direct and diffuse light, respectively (79 % direct light and 21 % diffuse light). The sun was a single object providing light in the direction of the corresponding location (Hannover, Germany, 52°23′N, 9°37′E) and time (at 1200 h on the dates of digitizing). The sky was approximated by an array of 72 directional light sources arranged in a hemisphere. For computing the light distribution a ray-tracer, integrated into *GroIMP*, was used with 10 million rays and a recursion depth of 10 reflections (Buck-Sorlin *et al.*, 2011). Leaf absorption, transmission and reflection of photosynthetically active radiation (PAR) were 87, 7 and 6 %, respectively (Kahlen *et al.*, 2008). The ground in the model (30 × 30m), above which the virtual canopy was constructed, was assumed to absorb 80 % and reflect 20 % of the incident PAR. Only the simulated results from the two plants in the middle of the middle row were taken for statistical analysis. Simulations for each digitized plant were

repeated 10 times, each run with a slight difference in plant orientation (±30°) in the virtual canopy. The intercepted PAR was used as input for the leaf photosynthesis model.

Modelling leaf photosynthesis

The measured ambient CO_2 concentration (C_a, ppm) temperature (°C) and water vapour pressure deficit (VPD) (D, kPa) in the greenhouses, together with the incoming PAR above the canopy (μmol m^{-2} s^{-1}), were used as environmental inputs for simulating leaf photosynthesis. Cucumber leaf photosynthesis was modelled by embedding the salinity effects on photosynthetic parameters (Chen *et al.*, 2015a) into a photosynthesis model for non-stressed conditions (Chen *et al.*, 2014a). All parameters and their values are listed in Supplementary Data Table S1.

In short, stomatal conductance, g_{sc}, was simulated as shown by Medlyn *et al.* (2011):

$$g_{sc} = g_0 + \left(1 + g_1 / \sqrt{D}\right) \cdot \left(A_{net} / C_a\right) \quad (1)$$

where g_0 and g_1 are the minimum stomatal conductance and an empirical parameter, respectively, and A_{net} (μmol CO_2 m^{-2} s^{-1}) is the minimum of the RuBP-regeneration-limited and Rubisco-carboxylation-limited photosynthesis rate (A_j and A_c, respectively, μmol CO_2 m^{-2} s^{-1}, Farquhar *et al.*, 1980):

$$A_c = V_{cmax}\left(C_c - \Gamma^*\right) / \left(C_c + K_c\left(1 + O / K_o\right)\right) - R_d \quad (2)$$

$$A_j = J \cdot \left(C_c - \Gamma^*\right) / \left(4C_c + 8\Gamma_*\right) - R_d \quad (3)$$

where V_{cmax} is the maximum rate of Rubisco carboxylation (μmol CO_2 m^{-2} s^{-1}), Γ^* is the CO_2 compensation point in the absence of dark respiration (for cucumber: 43.02 μmol mol^{-1}; Singsaas *et al.*, 2003), K_c (404 μmol mol^{-1}) and K_o (278 mmol mol^{-1}) are Michaelis–Menten constants of Rubisco for CO_2 and O_2, O (210 mmol mol^{-1}) is the mol fraction of O_2 at the site of carboxylation and R_d is the respiration rate. C_c (chloroplastic CO_2 concentration, μmol mol^{-1}) and J (electron transport rate, μmol $m^{-2}s^{-1}$) were calculated by:

$$C_c = C_a - \left(A_{net} / g_{sc}\right) - \left(A_{net} / g_m\right) \quad (4)$$

$$J = \left(\kappa_{2LL} \cdot I_{ab} + J_{max} - \sqrt{\left(\kappa_{2LL} \cdot I_{ab} + J_{max}\right)^2 - 4\theta \cdot J_{max} \cdot \kappa_{2LL} \cdot I_{ab}}\right) / (2\theta) \quad (5)$$

where g_m is mesophyll conductance (mol m^{-2} s^{-1}), I_{ab} is absorbed PAR (μmol photons m^{-2} s^{-1}) obtained from the ray-tracing light model and 3-D canopy model, J_{max} is the maximum electron transport rate (μmol e^- m^{-2} s^{-1}), κ_{2LL} and θ are constants describing the conversion efficiency of I_{ab} to J (0.425 mol e^- mol^{-1} photons) and convexity factor describing the response of J to I_{ab} (0.7), respectively. The dependency of V_{cmax}, J_{max}, g_m and R_d on leaf age is fitted to a log-normal curve (Irving and Robinson, 2006; Chen *et al.*, 2014a):

$$X_n(t) = X^{ref} \cdot \exp\left(-0.5\left(\log\left(t / t_{max}\right) / c_{sd}\right)^2\right) \quad (6)$$

where $X_n(t)$ is the photosynthetic variable on day t under non-stressed conditions, X^{ref} is the maximum of the variables, t_{max} is the time (day) when the X^{ref} occurs, and c_{sd} is curve standard deviation. Because of the good coordination between V_{cmax}, J_{max}, g_m and R_d (Egea *et al.*, 2011; Buckley *et al.*, 2013; Chen *et al.*, 2014a), t_{max} and c_{sd} for them are the same. Finally, A_j, A_c, g_{sc} and C_c were obtained by solving eqns (1)–(4) analytically. To avoid the discontinuity at the transition point between functions A_j and A_c, if the difference between A_j and A_c was smaller than 5 % of their average, photosynthesis was considered to be co-limited by both Rubisco-carboxylation and RuBP-regeneration rate (Yamori *et al.*, 2010, 2011). In this case, A_{net} is the interpolation between A_j and A_c, similar to other modelling studies (Peltoniemi *et al.*, 2012; Buckley *et al.*, 2013).

The effects of osmotic and ionic stresses on photosynthetic variables X are assumed to be additive and can be described by (Chen *et al.*, 2015a):

$$X_{stress}(t, S_s, S_l) = \left(1 + m_x S_s + n_x S_l\right) \cdot X_n(t) \quad (7)$$

where $X_{stress}(t)$ and $X_n(t)$ are the photosynthetic variables X (g_{sc}, g_m, V_{cmax} and J_{max}) under stressed and non-stressed conditions, respectively; S_s and S_l are the sodium concentrations in the nutrient solution and in the leaf water (mM), respectively; and m_x and n_x are empirical parameters for osmotic and ionic effects of salt, respectively. Temperature effects on photosynthetic parameters were taken from the literature (Sharkey *et al.*, 2007; Caemmerer and Evans, 2015).

Evaluation of the photosynthesis model

The 3rd and 8th leaves of the plants were measured using a portable gas exchange system (Li-6400; Licor) at C_a = 380 μmol mol^{-1}, leaf temperature = 25 °C, incoming light = 600 and 1300 μmol $m^{-2}s^{-1}$ (average daily light intensity and saturating light intensity, respectively) and relative humidity ≈ 65–70 %. Eight leaves per treatment were measured 3, 6, 9, 12, 15, 19 and 23 DAS. All measurements were conducted between 0900 and 1400 h. After gas exchange measurements, the measured part of the leaf was cut (approx.. 300 cm^2) and the fresh weight and cut area were recorded. Leaf samples were weighed after drying at 70 °C for 72 h for recording dry weight, then ground into fine powder. For sodium analysis, 50–100 mg of the powder was dry ashed at 500 °C and subsequently dissolved in nitric acid before being measured by an atom absorption spectrometer (1100B; Perkin Elmer, Waltham, MA, USA). Na^+ concentration in the leaf water (mM) was used as input for the photosynthesis model. Furthermore, Na^+ concentrations in leaves 3, 6, 8, 10, 13, 15, 18, 20, 23 and 25 were also measured on day 35 after the whole-plant harvest. The measured relationships between the time of a leaf grown under salinity (d) and Na^+ concentrations in that leaf (Supplementary Data Fig. S3) were used to estimate the Na^+ concentrations in leaves of the simulated canopies.

Disentangling the architectural and functional effects of salinity on canopy photosynthesis

Architectural limitations ($L_{A,x}$, %) and functional limitation ($L_{F,x}$, %) of salinity on cucumber canopy photosynthesis under x mM NaCl were quantified by (Chen *et al.*, 2015b):

$$L_{A,x} = \left(P_{c,0} - P_{c,ax}\right) / P_{c,0} \quad (8A)$$

$$L_{F,x} = \left(P_{c,ax} - P_{c,x}\right) / P_{c,0} \quad (8B)$$

where $P_{c,0}$, $P_{c,ax}$ and $P_{c,x}$ are the simulated whole plant photosynthesis rate (μmol per plant s^{-1}) of plants under non-stressed conditions, plants with *x* mM NaCl architecture but non-stressed photosynthetic capacity, and plants under *x* mM NaCl, respectively. Whole plant photosynthesis rate was the sum of photosynthesis from all leaves of the plants. The term $P_{c,0} - P_{c,ax}$ in eqn (8A) represents the difference in photosynthesis rates between stressed and non-stressed canopies having the same photosynthetic capacity but different size of the photosynthetic apparatus. Therefore, architectural limitations are a result of reduced leaf area and changed plant architecture under salinity. The term $P_{c,ax} - P_{c,x}$ in eqn (8B) represents the reduction of photosynthesis due to the salinity effects on photosynthetic function and is therefore defined as the functional limitations. Furthermore, canopy light interception efficiency (ε_i, unitless) and light use efficiency (ε_u) were calculated by:

$$\varepsilon_i = I_p D_p / I_{inc} \quad (9A)$$

$$\varepsilon_u = P_W / I_p \quad (9B)$$

where I_p is the light absorption per plant (μmol photon per plant s^{-1}), D_p is the plant density (plant m^{-2} ground area), I_{inc} is the total incoming radiation (μmol photon m^{-2} ground area s^{-1}) and P_W is the whole plant photosynthesis rate [$P_{c,x}$ in eqn (8), μmol per plant s^{-1}).

Quantitative limitation analyses at leaf level

The relative change of photosynthesis under RuBP-regeneration-limited (dA_j/A_j) and Rubisco-carboxylation-limited conditions (dA_c/A_c) can be described as (Chen *et al.*, 2015a)

$$dA_j / A_j = L_{sj} + L_{mj} + L_{bj} + L_{lj} = l_{sj} \cdot dg_{sc} / g_{sc} + l_{mj} \cdot dg_m / g_m + l_e \cdot J_{dB} / J + l_e \cdot J_{dI} / J \quad (10A)$$

$$dA_c / A_c = L_{sc} + L_{mc} + L_{bc} = l_{sc} \cdot dg_{sc} / g_{sc} + l_{mc} \cdot dg_m / g_m + l_{bc} \cdot dV_{cmax} / V_{cmax} \quad (10B)$$

where the subscripts j and c denote the RuBP-regeneration-limited and Rubisco-carboxylation-limited conditions, respectively; the subscripts s, m, b and l indicate the contributions of stomatal conductance, mesophyll conductance, biochemical capacity and light to photosynthetic limitation, respectively; l_s, l_m l_e and l_b are the *relative* limitations of stomatal and mesophyll conductance, electron transport rate and biochemical capacity, respectively; and J_{dB} and J_{dI} are the changes of electron transport rate due to biochemical capacity and irradiance, respectively. A complete description of eqns (10) can be found in Chen *et al.* (2015a). Under Rubisco-carboxylation and RuBP-regeneration co-limited conditions, limitations were calculated by the linear interpolation between L_j and L_c. Furthermore, we have noticed that using numerical integration of d*A* instead of partial differentiation of eqns (2) and (3), eqn (10) provides different results of dissecting photosynthetic limitations (Buckley and Diaz-Espejo, 2015). Therefore, systematic comparisons of the potential differences between both approaches were conducted using our data (see Supplementary Note S1).

Revised approach of quantitative limitation analyses at whole plant level

Whole plant photosynthetic limitation is the sum of the limitation of all leaves on a plant (Chen *et al.*, 2014a). For example, the stomatal limitation of a plant with *n* leaves (L_{sW}, μmol CO_2 per plant s^{-1}) can be calculated by:

$$L_{sW} = A_{max}^{ref} \cdot \sum_{k=1}^{n} L_{s,k} \cdot LA_k \quad (11)$$

where A_{max}^{ref} (μmol CO_2 m^{-2} s^{-1}) is the reference photosynthesis rate, calculated by assuming that all photosynthetic parameters reach their maxima simultaneously, LA_k is the area of leaf *k* (m^2) and $L_{s,k}$ is the stomatal limitation of leaf *k* (% of A_{max}^{ref}). L_{sW} represents the whole plant stomatal limitation. Since the magnitude of L_{sW} depends on the total leaf area of a plant, which differs between developmental stages and salinity levels, L_{sW} between salt treatments and developmental stages are not comparable. Therefore, the whole plant stomatal limitation was normalized by the whole plant leaf area:

$$L_{sP} = \left(A_{max}^{ref} \cdot \sum_{k=1}^{n} L_{s,k} \cdot LA_k\right) / \left(A_{max}^{ref} \cdot \sum_{k=1}^{n} LA_k\right) = \left(\sum_{k=1}^{n} L_{s,k} \cdot LA_k\right) / \left(\sum_{k=1}^{n} LA_k\right) \quad (12)$$

where L_{sP} represents the average of the whole plant stomatal limitation (%). Whole plant mesophyll (L_{mP}), biochemical (L_{bP}) and light (L_{lP}) limitations were calculated similarly. Using the experimental data, compositions of whole plant limitations were quantified for different salinity levels (0, 25 and 50 mM NaCl in the nutrient solution) and developmental stages (0, 7, 14, 21, 28 and 35 DAS). Moreover, sensitivity analyses of light intensity above the canopy were conducted. Since there were strong correlations between light environment and VPD, CO_2 concentration and air temperature (Supplementary Data Fig. S1), these correlations were considered for the sensitivity analyses. The photosynthesis model and all data processing were coded in *R* (v.3.3.0; R Foundation for Statistical Computing) to ensure the traceability of the analyses. These codes are available on demand.

RESULTS

Architectural and functional limitations of salinity

At the end of the experiment (35 DAS), measured shoot dry weights of plants grown under control (0 mM NaCl), low (25 mM NaCl) and high (50 mM NaCl) salinity were 291 ± 9, 223 ± 5 and 140 ± 5 g, respectively. This corresponded to a reduction in biomass by 23 % under low salinity and by 53 % under high salinity. By integrating the whole plant photosynthesis rate throughout the experimental period, our model predicted a 16 % reduction in canopy photosynthesis under 25 mM NaCl (Fig. 1A) and a 52 % reduction under 50 mM NaCl (Fig. 1B), similar to the measurements.

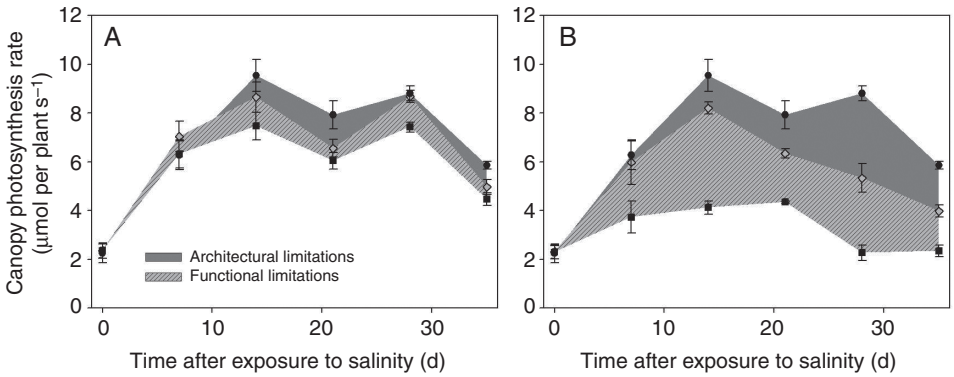

FIG. 1. Architectural limitations (dark grey area) and functional limitation (light grey filled with forward diagonal lines) of canopy photosynthesis rate under (A) 25 mM NaCl and (B) 50 mM NaCl conditions ($n = 3$, each replication represents the average value of 10 simulations). Black circles represent canopy photosynthesis under non-stressed conditions ($P_{c,0}$ in eqn 8); grey rhombuses represent photosynthesis rate of a canopy with architecture under stress but non-stressed photosynthetic capacity ($P_{c,ax}$ in eqn 8); black squares represent photosynthesis of the stressed canopy ($P_{c,x}$ in eqn 8).

This, together with the accurate plant digitizing (Table 1) and photosynthesis model at the leaf level (Supplementary Data Fig. S4), are the prerequisites for our interpretation of the experimental data by dissecting salinity effects into architectural and functional limitations. Integrated architectural and functional limitations throughout the experimental period (the dark grey area and the light grey area filled with forward diagonal lines in Fig. 1, respectively) were 6.3 and 9.9 % under low salinity and 19.9 and 32.2 % under high salinity, respectively.

Under both low and high salinity conditions, architectural limitations had similar magnitude to the reduction in size of photosynthetic apparatus (leaf area, Table 1, Fig. 2A). The reduction in light interception due to salinity (Fig. 3A) was related to the architectural limitations, but of a smaller magnitude under high salinity. After the start of salinity stress, functional limitations increased rapidly but fluctuated with time (Fig. 2B). Fluctuations of light use efficiency were also observed, which was due to the fluctuations in light intensity above the canopy (Fig. 3B). On the day when functional limitations were low (e.g. on 21 and 35 DAS), light use efficiency was high. Therefore, we tested the dependencies of functional and architectural limitations to the light intensity above the canopy by simulations using the canopy architecture of both salinity levels on 14, 21, 28 and 35 DAS. In general, architectural and functional limitations increased with light intensity above the canopy, but the increases in functional limitations with light were more drastic than those in architectural limitations (Fig. 4). For example, architectural limitations under low and high salinity were relatively constant (around 9 and 13 %, respectively) but functional limitations increased from 2 to 19 % and from 9 to 55 %, respectively (Fig. 4A). On 14 and 21 DAS, architectural limitations under high salinity were lower than functional limitations (Fig. 4A, B), but the reverse pattern was observed on 28 and 35 DAS (Fig. 4C, D).

TABLE 1. *Measured whole plant leaf area (LA, m^2)*

Day after salinity start	LA		
	0 mM NaCl	25 mM NaCl	50 mM NaCl
0*	0.27 ± 0.02	0.27 ± 0.02	0.27 ± 0.02
7*	0.66 ± 0.14	0.72 ± 0.10	0.56 ± 0.11
14*	1.56 ± 0.03	1.37 ± 0.11	1.18 ± 0.08
21*	2.07 ± 0.13	1.55 ± 0.11	1.36 ± 0.07
28*	2.02 ± 0.12	1.80 ± 0.09	1.06 ± 0.13
35*	2.10 ± 0.02	1.76 ± 0.03	1.07 ± 0.14
35†	2.16 ± 0.10	1.77 ± 0.06	0.94 ± 0.02

* Measured by plant digitizing.

† Measured by leaf area meter.

Salinity effects on the components of functional limitations – leaf level

Salinity enhanced the stomatal (L_s, Fig. 5A) and mesophyll limitation (L_m, Fig. 5B) of most leaves but decreased the light limitation (L_l, Fig. 5D). Salinity effects on biochemical limitation (L_b) depended on leaf age (Fig. 5C), light intensity (Fig. 6C) and developmental stage (Fig. S5). For example, on 21 DAS, low salinity increased L_s and L_m by 5–10 and 1–2 %, respectively, while high salinity reduced photosynthesis by 15–45 and 1–5 % due to stomatal and mesophyll limitation, respectively (Fig. 5A, B). The increase of L_b under salinity occurred only in the middle of the canopy (Fig. 5C).

Similar to the functional limitations at the plant level (Fig. 4), there were complex interactions between developmental stage, light intensity above the canopy and the different components of functional limitations (Fig. 6 and Supplementary Data Fig. S5). For example, on 21 DAS, stomatal limitation of the 15th leaves of the plants increased rapidly with light, especially under high salinity (Fig. 6A). Mesophyll limitations were less sensitive to light intensity (Fig. 6B). The negative effects of salinity on biochemical limitations were only significant under low light (Fig. 6C). Salinity reduced the light limitations (Fig. 6D).

Salinity effects on the components of functional limitations – whole plant level

At the whole plant level, the compositions of photosynthetic limitation changed with developmental stages and salinity levels. Under non-stressed conditions, whole plant stomatal (L_{sP}, Fig. 7A) and mesophyll limitation (L_{mP}, Fig. 7B) were

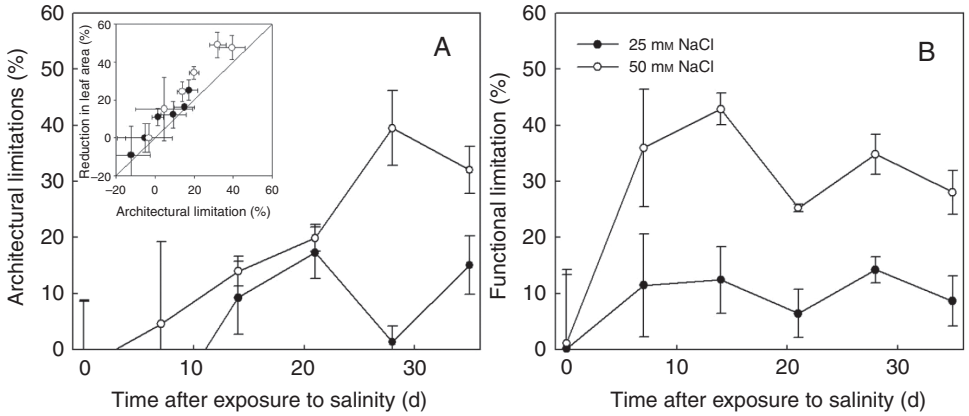

FIG. 2. Architectural limitations (A, $L_{A,x}$ in eqn 8) and functional limitation (B, L_{Fx} in eqn 8) of canopy photosynthesis rate under 25 mM NaCl (closed symbols) and 50 mM NaCl (open symbols), calculated from Fig. 1. The inset in A shows the relationship between architectural limitation and reduction in leaf area. The solid line in the inset represents a 1^:^1 line.

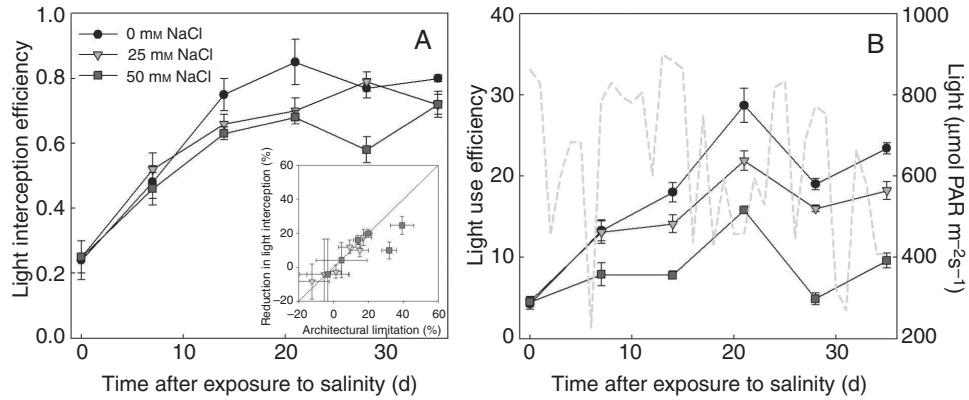

FIG. 3. Influence of salinity on (A) light interception efficiency (eqn 9A, unitless) and (B) light use effiency (eqn 9B, μmol CO_2 $mmol^{-1}$ photon). The light grey dashed line in B represents the daily average light environment outside the greenhouse condition, which was used for simulation. The inset in A shows the relationship between architectural limitation and reduction in light interception efficiency (n = 3, each replication represents the average value of 10 simulations). The solid line in the inset represents a 1^:^1 line.

low (around 10 and 3 %, respectively). In contrast to the small increases (5 %) in L_{sP} under low salinity, high salinity enhanced L_{sP} by more than 30 %. Low salinity effects on whole plant biochemical limitation (Fig. 7C) were small. The increase in biochemical limitations only occurred on 14 and 21 DAS under low salinity. Surprisingly, biochemical limitation under high salinity was smaller than control. Salinity stress reduced the whole plant light limitation (Fig. 7D), especially between 14 and 28 DAS. The dependencies of canopy photosynthetic limitations to the light condition above the canopy were similar to those of the 15th leaf in the canopy (Supplementary Data Fig. S6 and Fig. 6). In all components of the functional limitations, stomatal limitation increased most significantly with light intensity, indicating that the dependencies of functional limitation to light (Fig. 4) resulted from the stomatal limitation.

DISCUSSION

Although the salinity effects on photosynthesis at the leaf level have been studied for a long time in many different species (Drew *et al.*, 1990; Delfine *et al.*, 1999; Centritto *et al.*, 2003; James *et al.*, 2006; Tavakkoli *et al.*, 2010), there are very few data reporting salinity effects on whole plant photosynthesis or light use efficiency (but see Wang *et al.*, 2001; Qian and Fu, 2005). It is well known that salinity reduces whole plant photosynthesis but there is no study dissecting this reduction into different components related to physiological mechanisms. By using a dynamic FSPM of tomato, Chen *et al.* (2015b) separated functional limitations from the architectural limitations of canopy photosynthesis and found contrasting effects of stress combination (high temperature and salinity) on different traits. This work provides the methodological basis for separating architectural and functional limitations and proposed that an FSPM is the prerequisite for this separation. By combining experimental data and an FSPM, we provide a novel framework to dissect the salinity effects on canopy photosynthesis into architectural and functional limitations. This framework was combined with a quantitative limitation analysis of photosynthesis, which allowed further dissection of functional limitations into stomatal, mesophyll, biochemical and light limitations quantitatively (Chen *et al.*, 2014a). We further analysed the influences of light on the compositions of different limitations, because the different abiotic stresses, e.g. high light and

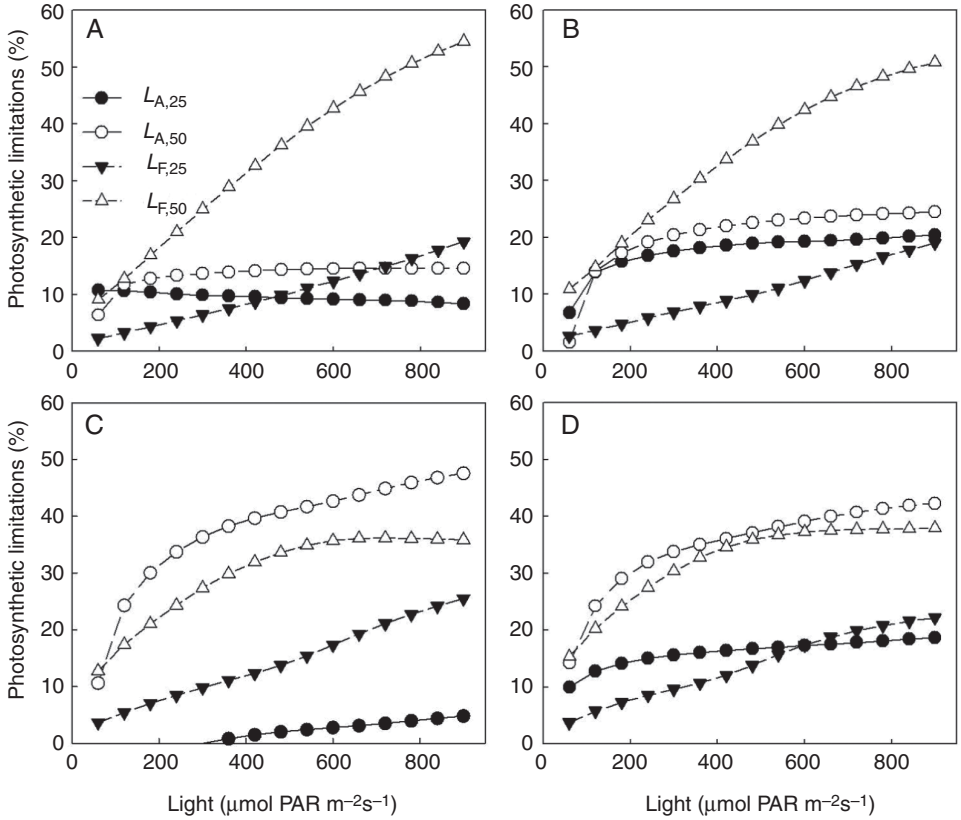

FIG. 4. Simulated dependencies of architectural and functional limitations ($L_{A,x}$ and $L_{F,x}$ in eqn 8, respectively) to light environment above the canopy on (A) 14, (B) 21, (C) 28 and (D) 35 d after salinity treatments. Closed symbols and open symbols represent 25 and 50 mM NaCl salinity, respectively. All values represent the average from three replicates.

salinity, may occur simultaneously under natural conditions, but the combined effects of multiple stresses are rarely studied (Suzuki *et al.*, 2014). These analyses may be used to identify the traits to be improved for salinity tolerance in cucumber and any other crop species.

Architectural and functional limitations are light-dependent

Both architectural and functional limitations showed strong dependencies on light (Fig. 4). The increasing salinity effects on instantaneous canopy photosynthesis rate with light resulted mainly from the increasing functional limitations, whereas this increase in architectural limitations was negligible between 200 and 1000 μmol PAR m^{-2} s^{-1} (Fig. 4). Two reasons might explain these dependencies. First, at the leaf level, there were drastic increases in stomatal limitations with light (Fig. 6A, Supplementary Data Fig. S5), as reported in the literature (Chen *et al.*, 2015a). This is due to the light effects on lowering C_c, which increases the relative stomatal limitation (l_s in eqn 10) and reduces the relative biochemical and light limitations (l_b and l_e in eqn 10; Chen *et al.*, 2015a). Second, VPD and temperature increased with the light conditions above the canopy in our simulations. According to eqn (1), high VPD reduces stomatal conductance and therefore increases stomatal limitations.

Under high salinity, architectural limitations increased continuously with time (Fig. 2A) and became higher than the functional limitations (Fig. 4C, D). Since the strongest reduction in leaf area occurred in the upper canopy (leaf ranks 15–25, data not shown), maintaining the elongation of young leaves, a trait related to osmotic tolerance (Rawson and Munns, 1984), is crucial for reducing architectural effects. The exact mechanisms and signal pathways controlling leaf growth under osmotic stress are still unclear (Munns and Tester, 2008; Roy *et al.*, 2014). Except for the osmotic effects on leaf area, leaf burn at the shoot tip in some plants under high salinity after a sunny day (in the greenhouse, PAR above the canopy could reach 1500 μmol m^{-2} s^{-1} at midday) further reduced leaf area. Such high light intensities, occurring together with high VPD and temperature, may have increased the transpirational demand of the upper canopy for leaf cooling and once the transpirational demand of a leaf is higher than its water supply, it will be overheated and injured. Since leaf burn was not observed in the plants under non-stress and low salinity level, it might have resulted from this salt-induced hydraulic failure of water transport. Under high salinity, the size and number of leaf veins may decrease (Hu *et al.*, 2005). These changes in vein anatomy may also modify the hydraulic supply capacity (Brodribb *et al.*, 2007), increase the vulnerability to cavitation (Comstock and Sperry, 2000) and then result in hydraulic failure. Both osmotic effects and leaf burn indicate that the negative architectural

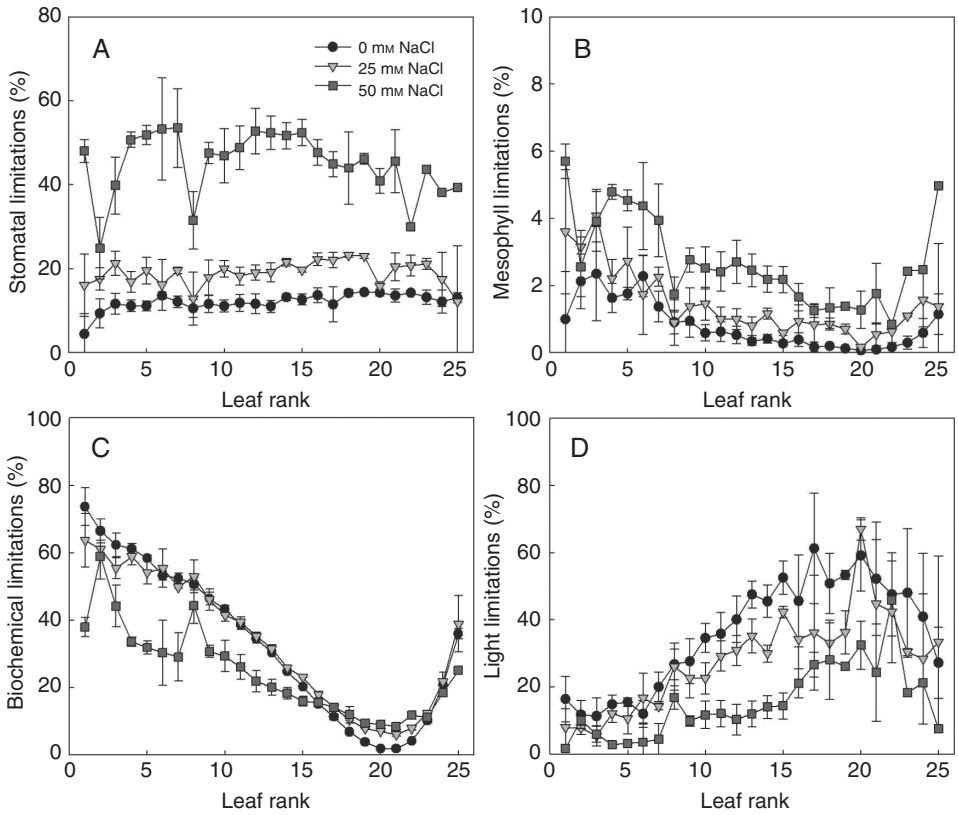

FIG. 5. Changes of (A) stomatal, (B) mesophyll, (C) biochemical and (D) light limitation with leaf rank and salinity level in the nutrient solution (circles, reverse triangles and squares represent additional 0, 25 and 50 mM NaCl in the nutrient solution, respectively) on day 21 after exposure to salinity ($n = 3$, each replication represents the average value of 10 simulations). Photosynthetically active radiation above the canopy was assumed to be 360 µmol photons m^{-2} s^{-1}. The leaves with higher leaf rank were the younger leaves in the canopy.

effects could be reduced by improving the hydraulic traits of the plant.

Methodological considerations on partitioning contributions to photosynthetic limitations

Recently, it has been proposed that using numerical integration instead of partial differentiation of eqns (2) and (3) (eqn 10) provides more accurate results of dissecting photosynthetic limitations (Buckley and Diaz-Espejo, 2015). Therefore, we compared the potential differences between both approaches systematically (see Supplementary Note S1) and found that errors of the partial differentiation approach were less than 4 %, while the potential errors of numerical integration approach could be up to 9 %. Both approaches have sufficient accuracy for a sound limitation analysis, but they mainly differ from partitioning the contributions of photosynthetic limitations into diffusional (CO_2 diffusion through stomata and mesophyll) or biochemical processes (Rubisco carboxylation or electron transport rate). The slightly higher errors of the numerical integration approach could be due to the fact that the Rubisco-carboxylation and RuBP-regeneration co-limited phase were not considered. This may introduce differences in reference photosynthesis rate by up to 10 % (data not shown). Furthermore, for partitioning the contribution of biochemical capacity (J_{max}) and light absorption (I_{ab}) to the limitation of electron transport rate, the approach proposed by Chen *et al.* (2014b) may mathematically (according to eqn 5) overestimate biochemical limitation (L_b) and underestimate light limitation (L_l), especially when J_{max} and I_{ab} of a leaf are far from their references (for detail, see Supplementary Note S1). This indicates that L_l at the lower canopy, where J_{max} and I_{ab} are low, may be more dominant than is suggested (Chen *et al.*, 2014a), encouraging news for greenhouse farmers using interlighting systems. For instance, based on the numerical integration approach, the light limitations at the lower canopy (ranks 1–10) under non-stressed conditions (Fig. 5) were 13 % higher than those calculated by the partial differentiation approach.

Even if there are potential discrepancies between the partial differentiation and numerical integration approaches and despite their different drawbacks, consensus exists on the functional limitations at the whole plant level. Firstly, processes related to electron transport contribute to the largest part of the limitation in a canopy under stress and non-stress conditions, similar to the analyses conducted at the leaf and canopy level in the non-stressed plants (Chen et al., 2014a, 2015a). Secondly, salinity reduced the absolute contributions of biochemical processes (Rubisco carboxylation or electron transport rate) to photosynthetic limitations (Figs 5C, D and 6C, D). This is due to the salinity effects on lowering C_c (Delfine *et al.*, 1999; Loreto *et al.*, 2003; Pérez-López *et al.*, 2012), which reduces the relative biochemical limitation (Chen *et al.*, 2015a).

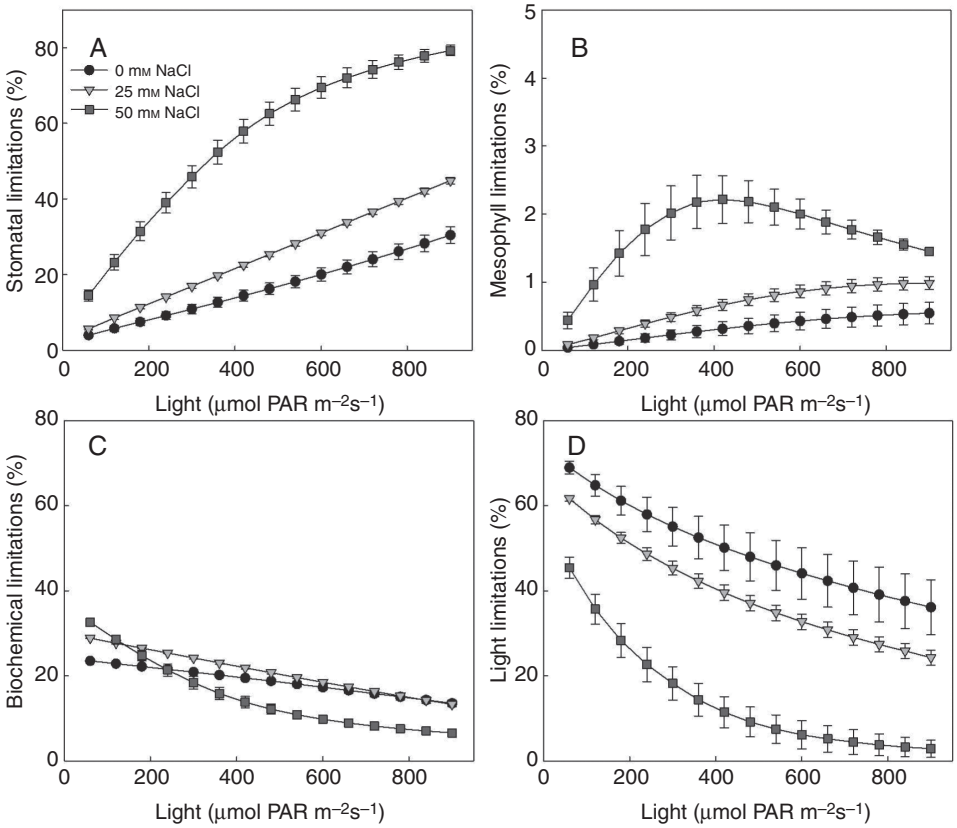

FIG. 6. Dependencies of (A) stomatal, (B) mesophyll, (C) biochemical and (D) light limitation to light environment above the canopy under different salinity levels (circles, reverse triangles and squares represent additional 0, 25 and 50 mM NaCl in the nutrient solution, respectively) on day 21 after exposure to salinity, leaf rank = 15 (n = 3, each replication represents the average value of 10 simulations). Similar dependencies of other leaf ranks can be found in Supplementary Data Fig. S5.

Therefore, the diffusional limitations (L_d, the sum of stomatal, L_s, and mesophyll, L_m, limitations) were the main contributions of salinity to photosynthetic limitations. Finally, the changes in photosynthetic limitations on 0 DAS are solely due to osmotic effects (Fig. 7A, B) and the increases in photosynthetic limitations on the following days can be considered as ionic effects. Therefore, ionic effects were the main contribution of L_s under high salinity, indicating the importance of stomatal regulation on reducing functional limitations. Importantly, although the empirical parameters t_{max} and c_{sd} in eqn (6) matched well to the observations from our cropping system and cucumber genotype in northern Germany, they may vary strongly between genotype (Khaembah *et al.*, 2013), nitrogen availability and environmental conditions (T-W. Chen *et al.*, unpublished data) and affect the model behaviours. A more mechanistic model describing the dynamic change of V_{cmax}, J_{max}, g_m and R_d would be a significant step for the future studies.

In summary, the present study used FSPM to interpret the experimental data by dissecting salinity effects on canopy photosynthesis into architectural and functional limitations. These analyses are helpful for disentangling the complex interactions between environmental conditions, plant structure and physiological function, and are especially suitable for studying multiple stress combinations. Our results highlight that the compositions of whole plant photosynthetic limitations under salinity are light-dependent and suggest that mechanisms related to leaf expansion and to stomatal regulation are the main factors limiting canopy photosynthesis under salinity.

SUPPLEMENTARY DATA

Supplementary data are available online at www.aob.oxfordjournals.org and consist of the following. Fig. S1. Variations in (A) daily average temperatures, vapour pressure deficit (VPD) and (B) ambient CO_2 concentration and light condition (photosynthetically active radiation, PAR) during the experiment (0700–2000 h). Fig. S2. Side view of the 3-D virtual cucumber canopies on day 0 (A) and day 14 (B) after exposure to 50 mM NaCl salinity. Fig. S3. Relationships between duration of the salinity treatment (day under salinity) and Na^+ concentrations in leaf water under 0 mM (A), 25 mM (B) and 50 mM (C) NaCl. Fig. S4. Measured and simulated photosynthesis rate (Anet 7, A) and stomatal conductance to CO_2 (gsc, B). Fig. S5. Dependencies of stomatal (SL), mesophyll (ML), biochemical (BL) and light (LL) limitations to light environment above the canopy (x-axes). Fig. S6. Dependencies of whole plant (A) stomatal, (B) mesophyll, (C) biochemical and (D) light limitation to light environment above the canopy under different salinity levels. Table S1. Parameter list of the photosynthesis model. Note S1: Evaluation of the quantitative limitation analysis using numerical integration and using partial differentiation.

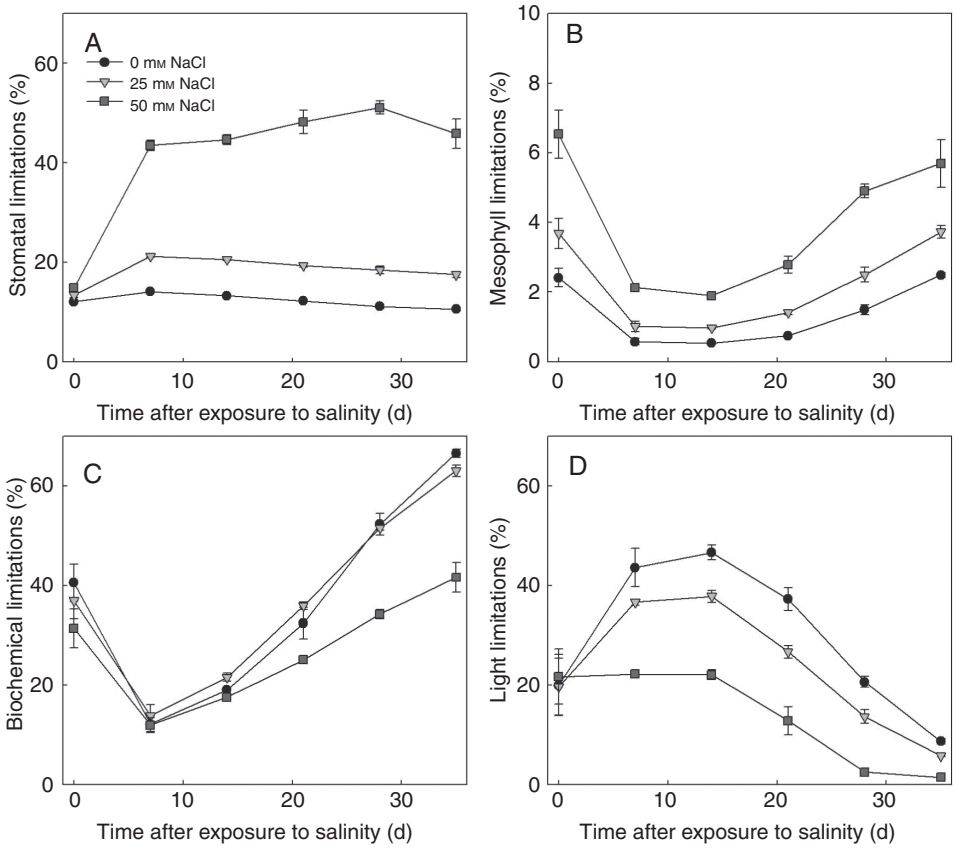

FIG. 7. Simulated canopy stomatal (A), mesophyll (B), biochemical (C) and light (D) limitations between days 0–35 after exposure to salinity ($n = 3$, each replication represents the average value of 10 simulations). Photosynthetically active radiation above the canopy was assumed to be 360 µmol photons m^{-2} s^{-1}.

ACKNOWLEDGEMENTS

This work was supported by Deutsche Forschungsgemeinschaft (DFG). The authors thank Ilona Napp for her help throughout the experiment, Melanie Kielenbeck, Marlena Klug and Emely Petersen for plant digitizing and sample preparation, Marie-Luise Lehmann for chemical analyses and Dr Michael Henke and Magnus Adler for their advices in programming the model.

LITERATURE CITED

Brodribb TJ, **Feild TS**, **Jordan GJ. 2007**. Leaf maximum photosynthetic rate and venation are linked by hydraulics. *Plant Physiology* **144**: 1890–1898.

Buckley T, **Diaz-Espejo A. 2015**. Partitioning changes in photosynthetic rate into contributions from different variables. *Plant Cell and Environment* **38**: 1200–1211.

Buckley TN, **Cescatti A**, **Farquhar G. 2013**. What does optimization theory actually predict about crown profiles of photosynthetic capacity when models incorporate greater realism? *Plant Cell and Environment* **36**: 1547–1563.

Buck-Sorlin G, **de Visser PH**, **Henke M**, et al. **2011**. Towards a functional–structural plant model of cut-rose: simulation of light environment, light absorption, photosynthesis and interference with the plant structure. *Annals of Botany* **108**: 1121–1134.

von Caemmerer S, **Evans JR. 2015**. Temperature responses of mesophyll conductance differ greatly between species. *Plant Cell and Environment* **38**: 629–637.

Cano F, **Sánchez-Gómez D**, **Rodríguez-Calcerrada J**, **Warren C**, **Gil L**, **Aranda I. 2013**. Effects of drought on mesophyll conductance and photosynthetic limitations at different tree canopy layers. *Plant Cell and Environment* **36**: 1961–1980.

Centritto M, **Loreto F**, **Chartzoulakis KS. 2003**. The use of low [CO_2] to estimate diffusional and non-diffusional limitations of photosynthetic capacity of salt-stressed olive saplings. *Plant Cell and Environment* **26**: 585–594.

Chen T, **Henke M**, **de Visser PHB**, **et al**. **2014*a***. What is the most prominent factor limiting photosynthesis in different layers of a greenhouse cucumber canopy? *Annals of Botany* **114**: 677–688.

Chen T, **Nguyen TMN**, **Kahlen K**, **Stützel H. 2014*b***. Quantification of the effects of architectural traits on dry mass production and light interception of tomato canopy under different temperature regimes using a dynamic functional-structural plant model. *Journal of Experimental Botany* **65**: 6399–6410.

Chen T, **Kahlen K**, **Stützel H. 2015*a***. Disentangling the contributions of osmotic and ionic effects of salinity on stomatal, mesophyll, biochemical and light limitations to photosynthesis. *Plant Cell and Environment* **38**: 1528–1542.

Chen T, **Nguyen TMN**, **Kahlen K**, **Stützel H. 2015*b***. High temperature and vapor pressure deficit aggravate architectural effects but ameliorate non-architectural effects of salinity on dry mass production of tomato. *Frontiers in Plant Science* **6**: 887.

Comstock JP, **Sperry JS. 2000**. Theoretical considerations of optimal conduit length for water transport in vascular plants. *New Phytologist* **148**: 195–218.

Delfine S, **Alvino A**, **Villani M**, **Loreto F. 1999**. Restrictions to carbon dioxide conductance and photosynthesis in spinach leaves recovering from salt stress. *Plant Physiology* **119**: 1101–1106.

Drew MC, **Hole PS**, **Picchioni GA. 1990**. Inhibition by NaCl of net CO_2 fixation and yield of cucumber. *Journal of American Society of Horticultural Science* **115**: 472–477.

Egea G, **González-Real MM**, **Baille A**, **Nortes PA**, **Diaz-Espejo A. 2011**. Disentangling the contributions of ontogeny and water stress to photosynthetic limitations in almond trees. *Plant Cell and Environment* **34**: 962–979.

Farquhar G, **von Caemmerer S**, **Berry J. 1980**. A biochemical model of photosynthetic CO_2 assimilation in leaves of C_3 species. *Planta* **149**: 78–90.

Flexas J, **Loreto F**, **Cornic G**, **Sharkey T. 2004**. Diffusive and metabolic limitations to photosynthesis under drought and salinity in C_3 plants. *Plant Biology* **6**: 269–279.

Flexas J, **Niinemets Ü**, **Gallé A**, et al. **2013**. Diffusional conductances to CO_2 as a target for increasing photosynthesis and photosynthetic water-use efficiency. *Photosynthesis Research* **117**: 45–59.

Grassi G, **Magnani F. 2005**. Stomatal, mesophyll conductance and biochemical limitations to photosynthesis as affected by drought and leaf ontogeny in ash and oak trees. *Plant Cell and Environment* **28**: 834–849.

Hu Y, **Fromm J**, **Schmidhalter U. 2005**. Effect of salinity on tissue architecture in expanding wheat leaves. *Planta* **220**: 838–848.

Irving LJ, **Robinson D. 2006**. A dynamic model of Rubisco turnover in cereal leaves. *New Phytologist* **169**: 493–504.

James RA, **Munns R**, **von Caemmerer S**, **Trejo C**, **Miller C**, **Condon T. 2006**. Photosynthetic capacity is related to the cellular and subcellular partitioning of Na^+, K^+ and Cl^- in salt-affected barley and durum wheat. *Plant Cell and Environment* **29**: 2185–2197.

Kahlen K, **Wiechers D**, **Stützel H. 2008**. Modelling leaf phototropism in a cucumber canopy. *Functional Plant Biology* **35**: 876.

Khaembah EN, **Irving LJ**, **Thom ER**, **Faville MJ**, **Easton HS**, **Matthew C. 2013**. Leaf Rubisco turnover in a perennial ryegrass (*Lolium perenne* L.) mapping population: genetic variation, identification of associated QTL, and correlation with plant morphology and yield. *Journal of Experimental Botany* **64**: 1305–1316.

Kniemeyer, O. 2008. *Design and implementation of a graph grammar based language for functional-structural plant modelling*. PhD thesis, BTU Cottbus, Germany.

Loreto F, **Centritto M**, **Chartzoulakis KS. 2003**. Photosynthetic limitations in olive cultivars with different sensitivity to salt stress. *Plant Cell and Environment* **26**: 595–601.

Medlyn BE, **Duursma RA**, **Eamus D**, et al. **2011**. Reconciling the optimal and empirical approaches to modelling stomatal conductance. *Global Change Biology* **17**: 2134–2144.

Munns R, **Tester M. 2008**. Mechanisms of salinity tolerance. *Annual Review in Plant Biology* **59**: 651–681.

Niinemets U. 2012. Optimization of foliage photosynthetic capacity in tree canopies: towards identifying missing constraints. *Tree Physiology* **32**: 505–509.

Peltoniemi MS, **Duursma RA**, **Medlyn BE. 2012**. Co-optimal distribution of leaf nitrogen and hydraulic conductance in plant canopies. *Tree Physiology* **32**: 510–519.

Pérez-López U, **Robredo A**, **Lacuesta M**, **Mena-Petite A**, **Muñoz-Rueda A. 2012**. Elevated CO_2 reduces stomatal and metabolic limitations on photosynthesis caused by salinity in ***Hordeum vulgare***. *Photosynthesis Research* **111**: 269–283.

Qian Y, **Fu J. 2005**. Response of creeping bentgrass to salinity and mowing management: carbohydrate availibility and ion accumulation. *HortScience* **40**: 2170–2174.

Rajendran K, **Tester M**, **Roy SJ. 2009**. Quantifying the three main components of salinity tolerance in cereals. *Plant Cell and Environment* **32**: 237–249.

Rawson H, **Munns R. 1984**. Leaf expansion in sunflower as influenced by salinity and short-term changes in carbon fixation. *Plant Cell and Environment* **7**: 207–213.

Roy SJ, **Negrão S**, **Tester M. 2014**. Salt resistant crop plants. *Current Opinion in Biotechnology* **26**: 115–124.

Savvas D, **Pappa V**, **Kotsiras A**, **Gizas G. 2005**. NaCl accumulation in a cucumber crop grown in a completely closed hydroponic system as influenced by NaCl concentration in irrigation water. *European Journal of Horticultural Science* **70**: 217–223.

Sharkey TD, **Bernacchi CJ**, **Farquhar GD**, **Singsaas EL. 2007**. Fitting photosynthetic carbon dioxide response curves for C_3 leaves. *Plant Cell and Environment* **30**: 1035–1040.

Singsaas E, **Ort D**, **Delucia E. 2003**. Elevated CO_2 effects on mesophyll conductance and its consequences for interpreting photosynthetic physiology. *Plant Cell and Environment* **27**: 41–50.

Stępień P, **Kłobus G. 2006**. Water relations and photosynthesis in ***Cucumis sativus*** L. leaves under salt stress. *Biologia Plantarum* **50**: 610–616.

Suzuki N, **Rivero RM**, **Shulaev V**, **Blumwald E**, **Mittler R. 2014**. Abiotic and biotic stress combinations. *New Phytologist* **203**: 32–43.

Tardieu F. 2012. Any trait or trait-related allele can confer drought tolerance: Just design the right drought scenario. *Journal of Experimental Botany* **63**: 25–31.

Tavakkoli E, **Rengasamy P**, **McDonald GK. 2010**. High concentrations of Na^+ and Cl^- ions in soil solution have simultaneous detrimental effects on growth of faba bean under salinity stress. *Journal of Experimental Botany* **61**: 4449–4459.

Wang D, **Shannon M**, **Grieve C. 2001**. Salinity reduces radiation absorption and use efficiency in soybean. *Field Crops Research* **69**: 267–277.

Wiechers D, **Kahlen K**, **Stützel H. 2011**. Evaluation of a radiosity based light model for greenhouse cucumber canopies. *Agricultural and Forest Meteorology* **151**: 906–915.

Yamori W, **Noguchi K**, **Hikosaka K**, **Terashima I. 2010**. Phenotypic plasticity in photosynthetic temperature acclimation among crop species with different cold tolerances. *Plant Physiology* **152**: 388–399.

Yamori W, **Nagai T**, **Makino A. 2011**. The rate-limiting step for CO_2 assimilation at different temperatures is influenced by the leaf nitrogen content in several C_3 crop species. *Plant Cell and Environment* **34**: 764–777.